ACOUSTIC COHERENCE IN A FLUCTUATING OCEAN: ANALYSIS OF THE 2016 ALMA CAMPAIGN.

Gaultier Real[a], Dominique Fattaccioli[a]

[a]DGA Techniques Navales, avenue de la Tour Royale, 83050 Toulon

gaultier.real@intradef.gouv.fr

Abstract: *The authors present the analysis of the acoustic propagation measurements conducted in November (7th-17th) 2016 near the shores of North East Corsica using the ALMA (Acoustic Laboratory for Marine Applications) system. The campaign is fully described in a companion paper (see Fattaccioli & Real, session "Design of new experimental facilities to address future problems in underwater acoustics"). The array consisted of 128 hydrophones arranged in a comblike configuration (4x32 vertical linear arrays). A moored pinger, 9 km from the arrays, transmitted signals with a 1 minute repetition rate. The study of the influence of fluctuations in the water column (typically internal waves, very frequent in shallow waters and coastal environments) on sound waves propagation is aimed.*
To do so, fluctuations of the received wavefronts at various frequencies (from 1kHz to 13kHz) on each of the four joint vertical linear arrays are shown. Statistics of the recorded data are also provided, including Mutual Coherence Function (MCF), radius of coherence and array gain degradation. The non-stationarity and non-uniformity of the received data highlights the influence of spatio-temporal variations of the medium.
In complement, CTD casts were performed at various times at the source and receiver locations. A CTD chain was deployed next to the receiving array so that environmental fluctuations are monitored during the campaign whole duration. The presence of a strong thermocline is shown by the data analysis.

Keywords: *at-sea experiment, propagation, acoustic coherence, fluctuations.*

1. INTRODUCTION

The document addresses the study of the data acquired during the 2016 ALMA at-sea measurements campaign. ALMA is a system that was presented in [1], and a companion paper [2] introduces its latest evolutions. It was originally designed in order to record signals in areas subject to environmental fluctuations, such as shallow and coastal waters. The influence of the variations of the physical parameters of the propagation medium, such as temperature and salinity, is a current topic of interest for researchers in underwater acoustic propagation [3-6]. Furthermore, a strong trend in signal processing studies is the research of corrective techniques allowing to mitigate the effect of wavefront distortions due to fluctuations of the environment [7-8 and the references within]. Various scientific fields (optics [9], medical imaging [10]) showed considerable advances in this specific domain, which is an additional motivation to provide field data in order to benchmark potential techniques allowing to achieve this goal in underwater acoustic data processing.

Furthermore, the validation of numerical models using at-sea measurements signals is also aimed by the ALMA system [11-12].

2. THE 2016 ALMA EXPERIMENT

2.1 Experimental Setup

The experiment was located near the shores of Campoloro, on eastern coast of the island of Corsica. On the receiving end, the passive array was deployed, along with its power supply and data recording buoy. The two are displayed respectively in red and yellow in Figure 1. About a mile east from the passive array, a thermistor string was deployed (in black in Figure 1). The length of the thermistor string was 150m, allowing to sample every 6.25 m the water temperature across the water depth. The acoustic pinger was moored 9 km south from the passive array at a 50m depth. The locations and depth of those elements are gathered in Table 1.

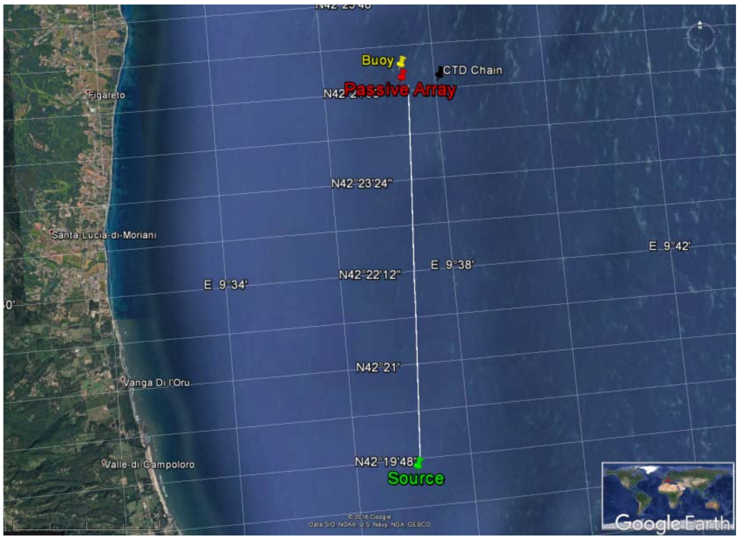

Figure 1. *ALMA 2016 Experiment Area*

Table 1. *Location and Depth of Experimental Equipment*

Points #	Description	Latitude	Longitude	Depth
P1	CTD Chain	42°24,670'N	9°38,049'E	0-150 m
P2	Buoy	42°24,866'N	9°37,366'E	0 m
P3	Passive Array	42°24,693'N	9°37,363'E	58-63 m
P4	Acoustic Source	42°19,656'N	9°37,004'E	50 m

The passive array was arranged in a comblike configuration: 4 vertical arrays of 32 hydrophones (acoustic sampling $\Delta h = 0.15\,m$, total acoustic height $H_a = 4.8m$) horizontally spaced by $\Delta S = 0.5m$). The overall dimensions of the array is $L = 2m \times H = 5m$. The arrays is schematically represented in Figure 2 (left) and a picture of the array on the deck of the ship is shown in Figure 2 (middle left). The omnidirectional wideband acoustic pinger is shown in Figure 2 (middle right); its buoy is also shows in the bottom right corner. Finally, the RBR thermistor string is shown is the top right corner of Figure 2.

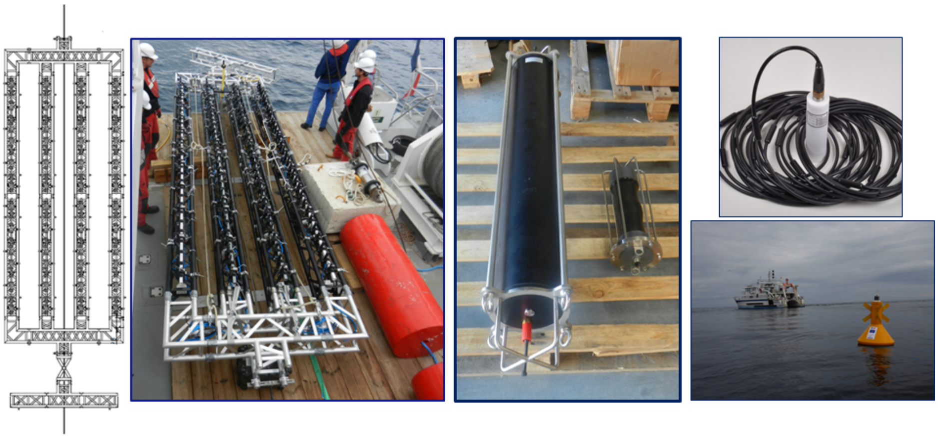

Figure 2. *Passive Array Arrangement (left)-Passive Array on the deck of the COMEX JANUS II ship (middle left) – ALSEAMAR's XXXX Acoustic Pinger (middle right) – RBR's Thermistor String (top right) – Source's Buoy and COMEX JANUS II (bottom right).*

The signal emitted was a sequence consisting of broadband pulses, frequency modulated signals, continuous waves (CW) and white noise, in the frequency range 1-13 kHz. The total duration of this sequence was $T_{seq} = 59s$, with a repetition rate of $T_r = 60s$.

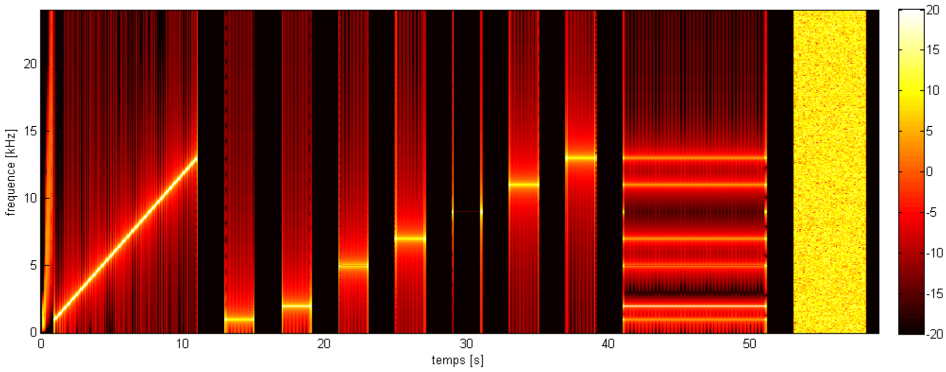

Figure 3. *Emitted Sequence.*

2.2 Environment

The thermistor string recorded temperature fluctuations throughout the entire duration of the campaign. Figure 4 displays the variation of the recorded temperature. Especially, the part of the experiment corresponding to the data analysis presented in section 3, denoted “Phase 9”, is highlighted below. The daily variation of temperature associated with the day and night cycle is clearly observed.

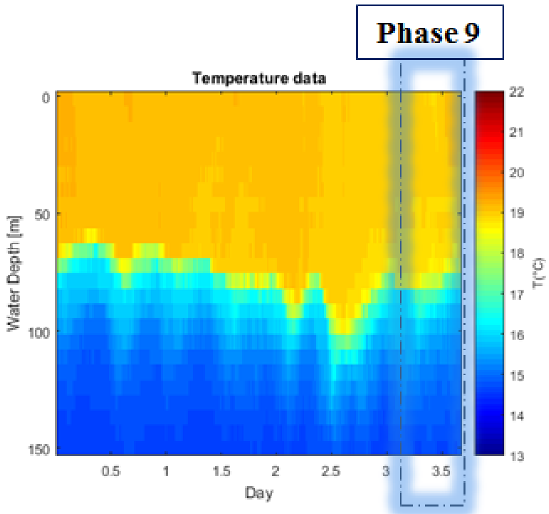

Figure 4. *Temperature data acquired by the CTD chain deployed in P1.*

In complement, CTD casts were performed at the source and receiver locations, at various times. The observed profiles are consistent with the thermistor string measurements. A strong thermocline, typical of this area at this season, is noticed. Thus, we can reasonably anticipate the presence of internal waves and their influence on the propagated signals.

3. EXPERIMENTAL RESULTS

In this section, we provide a glimpse of the first analysis of the data recorded during the campaign. Results corresponding to the last part of the experiment are presented here (“Phase 9”). We first show the fluctuations of the acoustic wavefront as a function of three parameters: space, time and frequency. We then provide the evaluation of the Mutual Coherence Function (MCF).

3.1 Acoustic Wavefront: Space, Time and Frequency Dependence.

Figures 5 to 7 display the received wavefront with the following organization: each VLA is displayed on 4 consecutive subplots. The vertical axis of each subplot is the hydrophone index, the horizontal axis is the time dependence (received ping index-each ping is emitted at T_r). Figure 5 shows the received wavefront at 1 kHz, Figure 6 shows the same quantity at 2 kHz and finally, Figure 7 shows it at 5 kHz.

These Figures exhibit remarkable time dependence since, in all cases, the received wavefront undergoes fluctuations. We especially observe a decrease in the acoustic level around ping #150. The high horizontal coherence is highlighted by the fact that the four VLAs exhibit very consistent patterns of fluctuation; nevertheless, the loss of vertical coherence is noted since the wavefront is not constant as a function of the hydrophone number, on each VLA. This analysis applies to all frequencies considered, but in particular, we note that an increase in frequency leads to a decrease in vertical coherence. In other words, the granularity of the received wavefront is much smaller at 5kHz than at 2kHz.

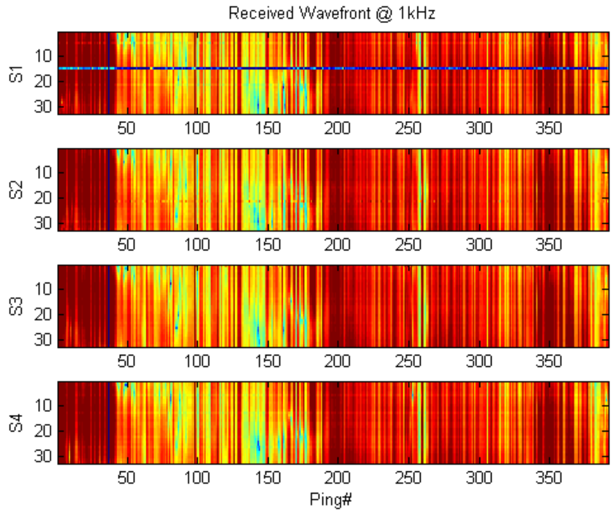

Figure 5. *Acoustic Wavefront Fluctuations at 1kHz.*

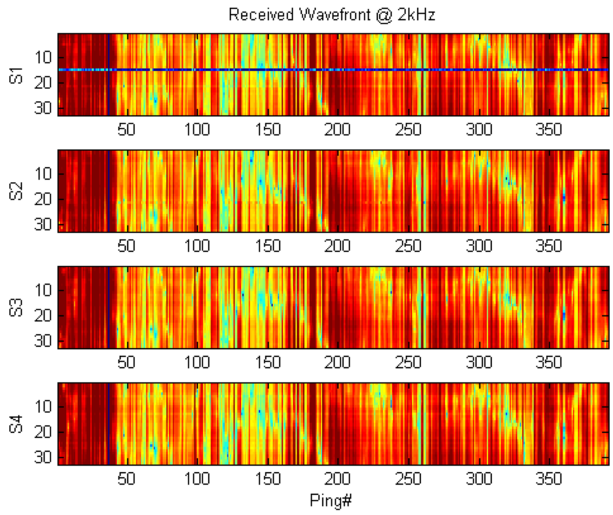

Figure 6. *Acoustic Wavefront Fluctuations at 2kHz.*

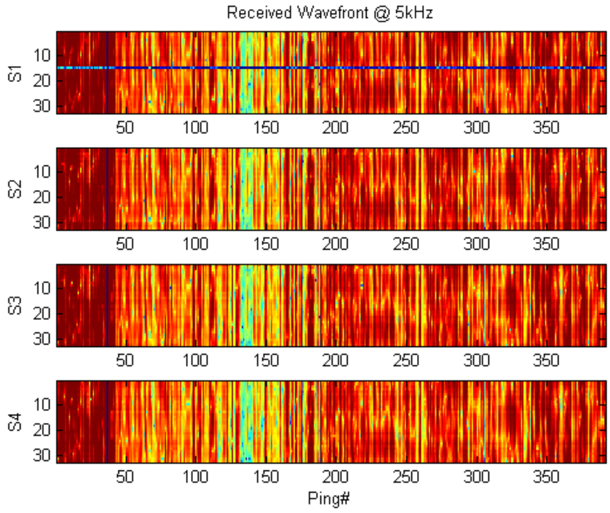

Figure 7. *Acoustic Wavefront Fluctuations at 5kHz.*

3.2 Mutual Coherence Function and Array Gain

The mutual coherence function (MCF) is calculated: it accounts for the spatial correlation of the acoustic wavefront along the vertical linear array. The MCF is calculated following[13-14]:

$$\Gamma(l) =<< \frac{\Pi(n)\Pi(n+l)}{|\Pi(n)||\Pi(n+l)|} >_N>_{N_R}$$

where Π is the complex received pressure in the Fourier domain (at frequency f0), n is the sensor index (N sensors total), N_R is the number of averaging and l is the sensor separation index. The loss of spatial correlation of the received waveforms is translated by the decrease of the MCF as a function of the sensor spacing (normalized by the wavelength in Figure 6). We observe, at all frequencies, a strong decrease of the MCF. The normalization by the wavelength leads the transition to be seen at the same point, however this can be measured by the radius of coherence (defined in [15] as the sensor spacing R_c such that $\Gamma(R_c) = e^{-1/2}$). The ratio of this value by the length of the array provides a significant metric, that we will call the effective coherence radius of the array. Figure 7 shows the value of the effective coherence radius as a function of the sound wave frequency. We observe that this parameter decreases with increasing frequency, confirming the idea that high frequency waves are more sensitive to environmental fluctuations.

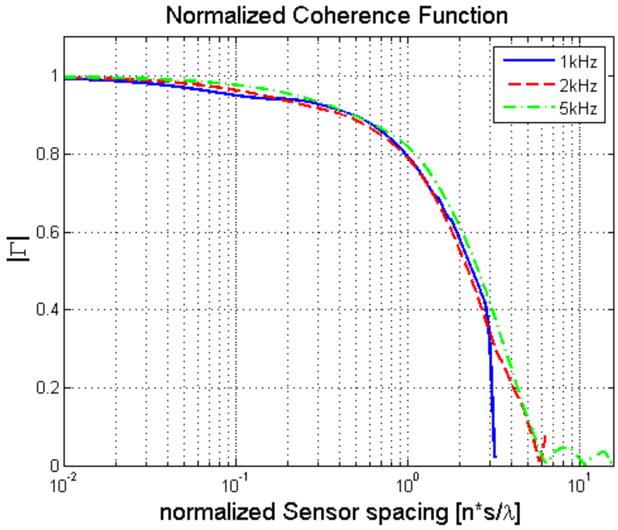

Figure 6. *MCF as a function of the normalized sensor spacing and the frequency.*

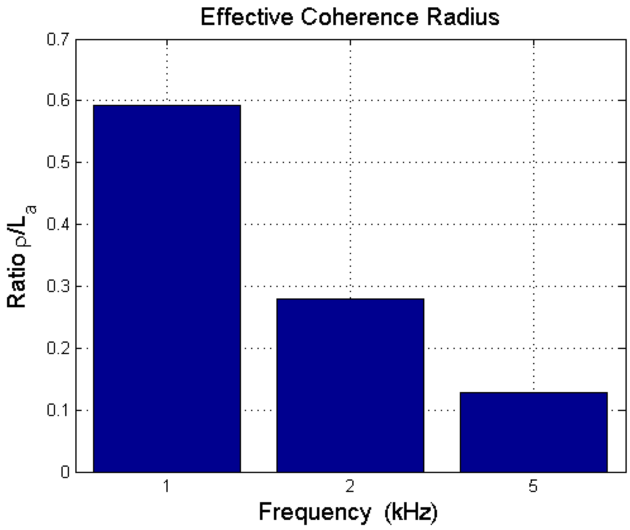

Figure 7. *Effective coherence radius as a function of the frequency.*

The loss of acoustic coherence translates into a degradation of the array gain. As depicted by Figure 7, the constructive information received by the array is reduced by the effects of fluctuations in the environment. Studies [15-18] relate the MCF and especially the radius of coherence to the degradation of the array gain, that we will note δAG. In Figure 8, we depict the AG as a function of the increasing number of sensors. The theoretical value of the AG ($G_{th} = 10\log(N)$) is also represented and is used to provide the measured δAG. The experimental δAG is compared to an empirical formula, provided in [19]. An excellent agreement is found at the two lowest frequencies, the frequency dependence of the array gain degradation is consistent with both the empirical formula and the measurements (see Figure 9).

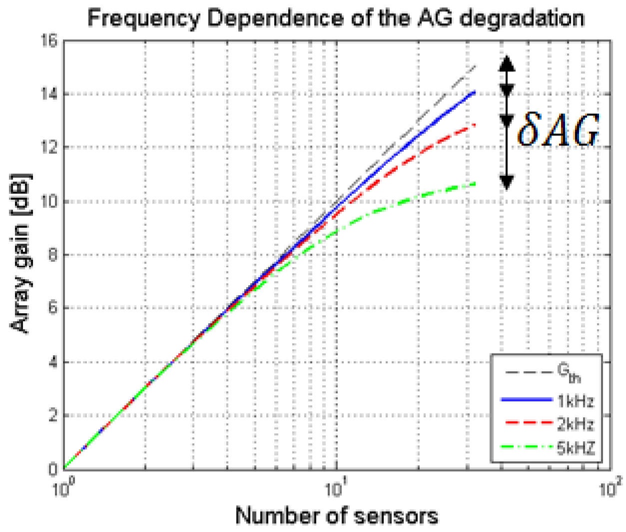

Figure 8. *Array Gain as a function of array size and frequency.*

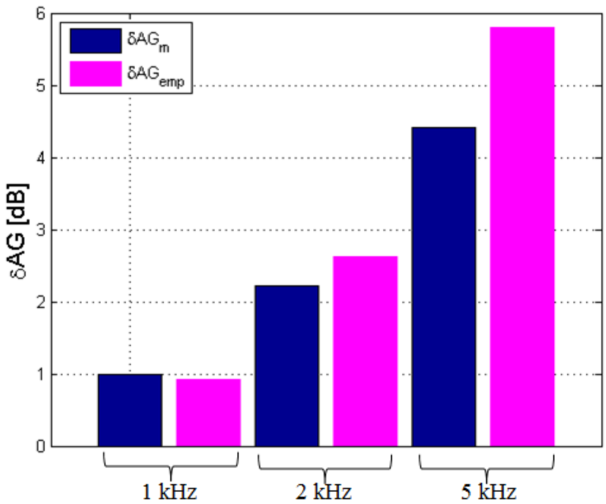

Figure 9. *Array Gain degradation: empirical formula vs measurements.*

4. CONCLUSION AND PERSPECTIVES

This paper presented the first analysis of sound signals received by a passive array composed of four segments of 32-element VLA. The acoustic wave was emitted by a pinger located 9km south of the array. A specific sequence was generated every two minutes. We focused here on the long CWs transmitted at 1, 2 and 5 kHz. The observation of the received acoustic wavefront displayed the non-stationarity over time, space and frequency of the signals. In fact, strong temporal fluctuations of the signal level are noticed over a 9 hours recording period. Moreover, the wavefront is not constant across the individual VLA, highlighting the loss of spatial coherence, more important with increasing frequency. A measurement of the radius of coherence and of the array gain degradation concurs with this conclusion.

More analyses of the huge amount of data collected are to come. Especially, a classification of the experimental configuration into regimes of fluctuation [3] can be attempted, using statistical tools such as the complex pressure distribution (or phasor) and the intensity distribution [18 and the references within]. Comparisons with oceanographic measurements and models would enforce the classification, with physical characteristics of internal waves fields. Moreover, the signals acquired can be used in order to benchmark techniques of wavefront correction, with the inner goal of an “environmental adaptative” sonar.

REFERENCES

[1] **Fattaccioli, D.** Alma: a new experimental acoustic system to explore coastal waters, *Proceedings of the 3rd Underwater Acoustic Conference and Exhibition*, Chania, Greece, pp. 1-6, 2015.

[2] **Fattaccioli, D. and Real, G.** The DGA “ALMA” Project: an overview of the recent improvements of the system capabilities and of the at-sea campaign ALMA-2016, *Proceedings of the 4th Underwater Acoustic Conference and Exhibition*, Skiathos, Greece, pp. 1-6, 2017.

[3] **Dashen, R., Munk, W. H., & Watson, K. M.** (2010). *Sound transmission through a fluctuating ocean*. Cambridge University Press.

[4] **Lynch, J. F., Lin, Y. T., Duda, T. F., & Newhall, A. E.** (2010). Acoustic ducting, reflection, refraction, and dispersion by curved nonlinear internal waves in shallow water. *IEEE Journal of Oceanic Engineering*, *35*(1), 12-27.

[5] **Colosi, J. A.** (2016). *Sound Propagation through the Stochastic Ocean*. Cambridge University Press.

[6] **Duda, T. F., Flatté, S. M., Colosi, J. A., Cornuelle, B. D., Hildebrand, J. A., Hodgkiss Jr, W. S., ... & Spindel, R. C.** (1992). Measured wave-front fluctuations in 1000-km pulse propagation in the Pacific Ocean. *The Journal of the Acoustical Society of America*, 92(2), 939-955.

[7] **Real, G., Cristol, X., Habault, D. & Fattaccioli, D.** Mitigation of decoherence effects in passive sonar : application to a scaled experiment, *Proceedings of the Acoustic and Environmental Variability, Fluctuations and Coherence Workshop,* Cambridge, UK, pp. 1-8; 2016.

[8] **Lefort, R., Real, G., & Drémeau, A.** (2017). Direct regressions for underwater acoustic source localization in fluctuating oceans. *Applied Acoustics*, *116*, 303-310.

[9] **Beckers, J. M.** (1993). Adaptive optics for astronomy: principles, performance, and applications. Annual review of astronomy and astrophysics, 31(1), 13-62.

[10] **Hinkelman, L. M., Liu, D. L., Waag, R. C., Zhu, Q., & Steinberg, B. D.** (1995). Measurement and correction of ultrasonic pulse distortion produced by the human breast. *The Journal of the Acoustical Society of America*, *97*(3), 1958-1969.

[11] **Cristol, X., Real, G., Fattaccioli, D. & Chalindar, B.** ALMA 2014: Observations of multiple scattering from random inhomogeneities transported by a mean flow, *Proceedings of the 4th Underwater Acoustic Conference and Exhibition*, Skiathos, Greece, pp. 1-6, 2017.

[12] **Real, G., Cristol, X., Habault, D. & Fattaccioli, D.** Decoherence effects in 3D fluctuating environments: Numerical and experimental study, *Proceedings of Meetings on Acoustics, Acoustical Society of America Meeting*, Boston, USA, pp.1-8,2017.

[13] **Collis, J. M., Duda, T. F., Lynch, J. F., & DeFerrari, H. A.** (2008). Observed limiting cases of horizontal field coherence and array performance in a time-varying internal wavefield. *The Journal of the Acoustical Society of America*, *124*(3), EL97-EL103.

[14] **Carey, W. M., Lynch, J. F., Siegmann, W. L., Rozenfeld, I., & Sperry, B. J.** (2006). Sound transmission and spatial coherence in selected shallow-water areas: Measurements and theory. *Journal of Computational Acoustics*, *14*(02), 265-298.

[15] **Carey, W. M.** (1998). The determination of signal coherence length based on signal coherence and gain measurements in deep and shallow water. *The Journal of the Acoustical Society of America*, *104*(2), 831-837.

[16] **Gorodetskaya, E. Y., Malekhanov, A. I., Sazontov, A. G., & Vdovicheva, N. K.** (1999). Deep-water acoustic coherence at long ranges: Theoretical prediction and effects on large-array signal processing. *IEEE journal of oceanic engineering*, *24*(2), 156-171.

[17] **Real, G., Cristol, X., Habault, D., Sessarego, J. P., & Fattaccioli, D.** (2015). Influence of de-coherence effects on sonar array gain: scaled experiment, simulations and simplified theory comparison, *Proceedings of the 3rd Underwater Acoustic Conference and Exhibition*, Chania, Greece, pp. 1-6, 2015.

[18] **Real, G.** (2015). An ultrasonic testbench for reproducing the degradation of sonar performance in a fluctuating ocean (Doctoral dissertation, LMA CNRS UPR 7051).

[19] **Fattaccioli, D., Cristol, X., Destelan, G. P., & Danet, P.** (2009). Sonar processing performance in random environments. *Proceedings Of Underwater Acoustic Measurements (UAM 09), Nafplion, Greece*, 21-26.